Appl Nanosci (2012) 2:25–30
DOI 10.1007/s13204-011-0035-y

ORIGINAL ARTICLE

The photoelectronic behaviors of MoO_3-loaded ZrO_2/carbon cluster nanocomposite materials

H. Matsui · A. Ishiko · S. Karuppuchamy · M. A. Hassan · M. Yoshihara

Received: 30 June 2011 / Accepted: 16 September 2011 / Published online: 30 September 2011

Abstract A novel nano-sized ZrO_2/carbon cluster composite materials (I_c's) were successfully obtained by the calcination of $ZrCl_4$/starch complexes I's under an argon atmosphere. Pt- and/or MoO_3-loaded ZrO_2/carbon clusters composite materials were also prepared by doping Pt and/or MoO_3 particles on the surface of I_c's. The surface characterization of the composite materials was carried out using transmission electron microscopy (TEM). The TEM observation of the materials showed the presence of particles with the diameters of a few nanometers, possibly Pt particles, and of 50–100 nm, possibly MoO_3 particles, in the matrix. Pt- and/or MoO_3-loaded ZrO_2/carbon cluster composite materials show the efficient photocatalytic activity under visible light irradiation.

Keywords Composites · Nano materials · Nanostructure · Sensitization

Introduction

Construction of a stable charge-separated electron excitation under visible light irradiation is required for achieving an artificial photosynthesis function, and semiconductors have been expected to provide such a function (Fujihara et al. 1998; Domen et al. 2000; Konta et al. 2004; Kudo et al. 2004; Kobayashi et al. 2005; Aki et al. 2006). Effective oxidation–reduction function will be achieved by increasing the stability of charge separation state without the recombination of holes and excited electrons. We have assumed that the calcination of metal–organic hybrid materials will provide new types of nano-sized metal compound-carbon clusters composite materials, in which some bonding on the interfaces of carbon clusters and metal compounds will be formed. The bonding on the interfaces of carbon clusters and metal compounds may affect the natures of band gaps and/or electron transfer, and carbon clusters will enhance the light absorption ability (Yamamoto et al. 2006; Matsui et al. 2007a; Furukawa et al. 2007; Kawahara et al. 2007a; Matsui et al. 2007b; Kawahara et al. 2007b; Miyazaki et al. 2008; Matsui et al. 2009a). We have thus been examining to clarify the electron transfer feature of various metal/oxides carbon clusters composite materials (Miyazaki et al. 2009a, b; Matsui et al. 2009b; Ge et al. 2010; Zhang et al. 2010).

In the previous paper, we showed the electronic behaviors of MoO_3/carbon clusters/ZrO_2 composite materials obtained by the microwave treatment of $MoCl_5$/$ZrCl_4$/starch/graphite complexes, and the photo-responsive catalysis with an electron transfer process of MoO_3 → carbon clusters → ZrO_2 was shown to take place (Kawahara et al. 2007b). Here, we considered that MoO_3-loading onto carbon clusters/ZrO_2 composite material could cause an effective and/or selective electron transfer feature. In the present work, nano-sized MoO_3 particles were modified on ZrO_2/carbon clusters composite materials I_c's which were obtained by the calcination of $ZrCl_4$/starch complexes I's (Scheme 1). The electronic feature and photo-catalytic activities of Pt- and/or MoO_3-loaded ZrO_2/carbon clusters composite materials were also investigated under visible light irradiation.

H. Matsui · A. Ishiko · M. Yoshihara
Department of Applied Chemistry, Faculty of Science and Engineering, Kinki University, 3-4-1, Kowakae, Higashiosaka, Osaka 577-8502, Japan

S. Karuppuchamy (✉) · M. A. Hassan
Institute of Bioscience, Universiti Putra Malaysia, 43400 Serdang, Selangor, Malaysia
e-mail: skchamy@ibs.upm.edu.my

Scheme 1 Synthesis of the materials

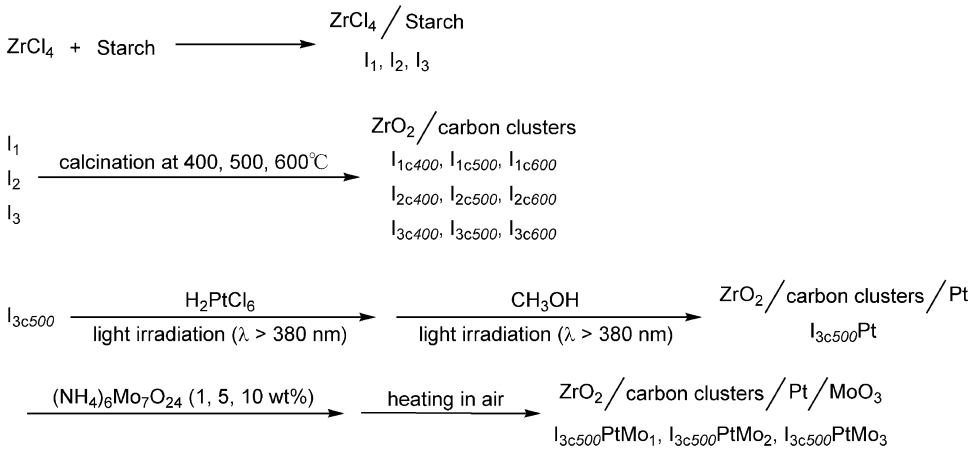

Experimental

Reagents

Commercially available zirconium chloride $ZrCl_4$, hexaammonium heptamolybdate tetrahydrate $(NH_4)_6Mo_7O_{24}\cdot 4H_2O$, starch, methylene blue, citric acid, hydrogen hexachloroplatinate hexahydrate $H_2PtCl_6\cdot 6H_2O$, and potassium permanganate were used as received.

Synthesis of complexes I's

A mixture of $ZrCl_4$ and starch in 300 mL of distilled water was stirred at room temperature for 1 h. Then the water was evaporated under a reduced pressure and subsequently, the residues were dried under vacuum to obtain complexes I's. The amounts of reagents used for the synthesis are shown in Table 1.

Calcination of complexes I's

3 g of I_1, I_2 and I_3 in porcelain crucible was heated under an argon atmosphere with a heating rate of 5°C/min and kept at 400, 500, and 600°C for 1 h to obtain calcined materials I_{1c400}–I_{1c600}, I_{2c400}–I_{2c600} and I_{3c400}–I_{3c600}, respectively.

Table 1 Charged amounts of reagents for preparing complexes I_1, I_2 and I_3

Materials	g (mmol)		Ratios
	Starch	$ZrCl_4$	[Starch]/[$ZrCl_4$]
I_1	25.5 (156.3)	4.5 (19.3)	8.1
I_2	26.9 (164.9)	3.1 (13.3)	12.4
I_3	27.6 (169.2)	2.4 (10.3)	16.4

Pt-loading on I_{3c500}

A mixture of 0.1 g of I_{3c500} and 0.5 mL of an aqueous 4.99 mmol/L hydrogen hexachloroplainate solution was irradiated by light ($\lambda > 380$ nm) with stirring for 30 min. 0.5 mL of methanol was added to the mixture and subsequently the resulting mixture was again irradiated by light ($\lambda > 380$ nm) with stirring for 30 min. The precipitates were collected, washed with distilled water, and dried under a vacuum to obtain Pt-loaded material denoted as I_{3c500}Pt.

MoO_3-loading on I_{3c500}Pt

A mixture of 50 mg of I_{3c500}Pt and 0.62 mg (0.5 μmol), 3.13 mg (2.5 μmol) and/or 6.26 mg (5.01 μmol) of $(NH_4)_6Mo_7O_{24}\cdot 4H_2O$ in 100 mL of distilled water was stirred at room temperature for 24 h. Water was evaporated under vacuum to yield the precipitates, which were dried and calcined in a porcelain crucible in the air at 300°C for 10 min using a Barnstead Thermolyne FB1300 electric furnace to obtain MoO_3-loaded materials denoted as I_{3c500}PtMo's, i.e., I_{3c500}PtMo$_1$, I_{3c500}PtMo$_2$ and/or I_{3c500}PtMo$_3$, respectively.

MoO_3-modification on I_{3c500}

A mixture of 50 mg of I_{3c500} and 6.26 mg (5.01 μmol) of $(NH_4)_6Mo_7O_{24}\cdot 4H_2O$ in 100 mL of distilled water was stirred at room temperature for 24 h. Water was evaporated to obtain the precipitates, which were then dried and calcined in a porcelain crucible in the air at 300°C for 10 min to yield MoO_3-loaded material denoted as I_{3c500}Mo.

Pt-loading on I_{3c500}Mo

A mixture of 0.1 g of I_{3c500}Mo and 0.5 mL of an aqueous 4.99 mmol/L hydrogen hexachloroplatinate solution was

then treated by the similar procedure described in "Pt-loading on I_{3c500}" to obtain Pt-loaded material denoted as I_{3c500}MoPt.

MnO_2-loading on I_{3c500}Pt

A mixture of 50 mg of I_{3c500}Pt, 0.08 mg (0.5 μmol) of $KMnO_4$ and 3 mL of ethanol in 100 mL of distilled water was stirred at room temperature for 24 h. Water was evaporated, and subsequently the residues were dried and calcined in a porcelain crucible in the air at 300°C for 30 min to obtain MnO_2-loaded material denoted as I_{3c500}PtMn.

Characterization

Elemental analyses were performed for C and H using Yanaco MT-6, and for Zr, Mo and Pt using Shimadzu ICPS-7500. XPS analyses were done using Shimadzu ESCA-850. TEM observations were carried out using Jeol JEM-3010. ESR spectra were measured using Jeol JEM-3010. TCD gas chromatography was taken with Shimadzu GC-8A. Visible light was generated using a Hoya-Schott Megalight 100 halogen lamp. UV–Vis spectra were measured using Hitachi U-4000. The reduction reaction of meyhylene blue with the calcined materials was carried out in the following way. 3 mg of the calcined materials was added into 10 mL of a 0.03 mmol/L methylene blue-0.12 mmol/l citric acid aqueous solution and the mixture was stirred in the dark for 48 h. The mixture was irradiated with visible light ($\lambda > 460$ nm) and the concentration of methylene blue was estimated by UV–Vis spectral analysis.

The oxidation–reduction reaction of an aqueous silver nitrate solution with the calcined materials was also performed in the following way. A mixture of 10 mg of the materials and 1 mL of an aqueous 0.05 mmol/L $AgNO_3$ solution was irradiated by visible light (>460 nm) under an argon atmosphere for 3 h, and the evolved O_2 gas was analyzed with gas chromatography and the formed Ag was estimated by ICP analysis.

Water photo-decomposition reaction with the calcined materials was carried out in the following way. 10 mg of the materials in 0.2 mL of degassed water was irradiated by visible light ($\lambda > 460$ nm) at room temperature for 12 h under an argon atmosphere, and the evolved H_2 and O_2 gases were analyzed by gas chromatography.

Results and discussion

The results of the elemental analyses of complexes I_1–I_3 are shown in Table 2. Zr atom was detected in the complexes. The SEM–EDX measurements of the complexes showed that Zr atom was uniformly dispersed in the materials. The calcination of complexes I's produced black-colored materials I_c's. Table 2 also summarizes the results of the elemental analyses of the calcined materials. The observed H contents decreased with the increase of the calcination temperature, suggesting that the carbonization of the materials proceeded. [C]/[Zr] ratios in the calcined materials increased with the increase of [Starch]/[$ZrCl_4$] ratios in the complexes. The XPS measurements of the calcined materials showed peaks at 182.0–182.3 eV due to the Zr_{3d} orbital of ZrO_2. The TEM observations revealed the presence of particles, possibly ZrO_2, with the diameters of 3–5 nm for I_{1c500} and of 2–3 nm for I_{2c500} and I_{3c500} (Fig. 1). The results suggest that the calcined materials were composed of nano-sized ZrO_2 and carbon clusters.

Table 2 Elemental analysis of complexes I_1–I_3 and calcined materials I_{1c}s–I_{3c}s

Materials	C (%)	H (%)	Zr (%)	[C]/[Zr]
I_1	33.65	5.92	4.32	44
I_{1c400}	60.23	3.12	11.3	40
I_{1c500}	67.21	2.87	13.3	38
I_{1c600}	67.41	2.20	13.1	39
I_2	33.99	5.75	3.53	74
I_{2c400}	71.54	3.12	10.6	51
I_{2c500}	68.88	2.90	10.3	50
I_{2c600}	77.40	1.99	11.5	51
I_3	35.67	5.93	2.82	96
I_{3c400}	71.82	3.20	8.00	68
I_{3c500}	69.03	3.15	8.31	63
I_{3c600}	73.48	1.62	9.50	58

In order to examine the electron transfer process of the calcined materials, the ESR spectra of I_{3c400} in the presence of either an oxidant (1,4-benzoquinone) or a reductant (1,4-hydroquinone) under the irradiation of visible light ($\lambda > 460$ nm) were measured (Fig. 2). A peak at 337 mT ($g = 2.003$) was found to increase with the addition of the oxidant and decrease with the addition of the reductant, indicating that the signal is due to a cation radical. Our opinion is that a visible light-sensitive electron transfer in the process of carbon clusters → ZrO_2 took place to form an oxidation site at the carbon clusters and a reduction site at the ZrO_2 parts.

The photo-catalytic abilities of the calcined materials were examined. Figure 3 is the UV–Vis spectra of methylene blue in the presence of I_{3c500} under visible light (>460 nm) irradiation. The absorption peak intensity of methylene blue was found to decrease with the irradiation time, indicating that I_{3c500} had photo-responsive reduction ability. The reduction activities (ra) of the calcined

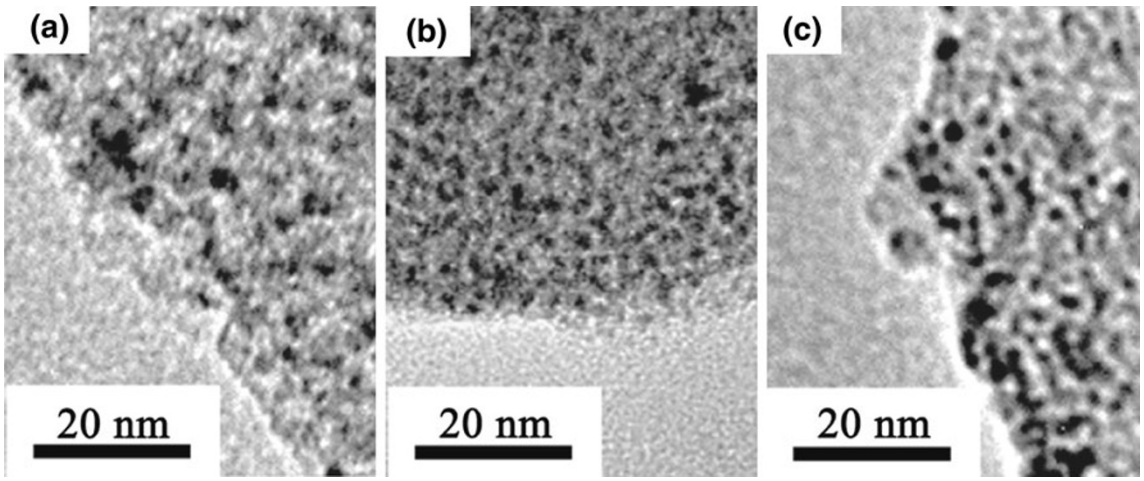

Fig. 1 TEM images of I_{1c500}, I_{2c500} and I_{3c500}

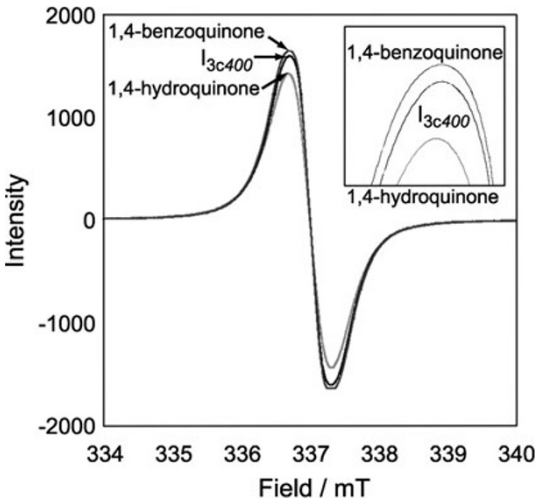

Fig. 2 ESR spectra of I_{3c400} in the presence of either 1,4-benzoquinone or 1,4-hydroquinone under the irradiation of visible light ($\lambda > 460$ nm)

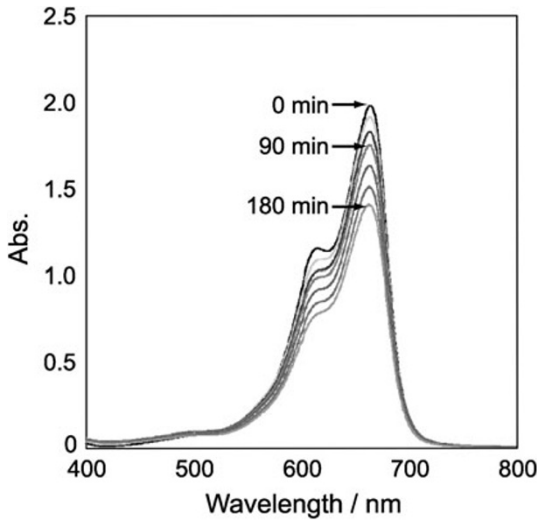

Fig. 3 UV–Visible spectra of methylene blue in the presence of I_{3c500} under the irradiation of visible light ($\lambda > 460$ nm)

materials were determined by the equation ra = (the amount of methylene blue) × (g of the calcined material)$^{-1}$ × (hour)$^{-1}$ and the results are shown in Table 3. The highest ra value was observed for I_{3c500}, indicating that I_{3c500} had the highest reduction ability.

The surface of I_{3c500} was modified with Pt particles according to the procedure described in "Pt-loading on I_{3c500}" to yield Pt-loaded material I_{3c500}Pt. Subsequently I_{3c500}Pt was also modified with MoO_3 according to the method described in "MoO_3-loading on I_{3c500}Pt" to obtain MoO_3-loaded materials I_{3c500}PtMo's. The results of the elemental analyses of I_{3c500}Pt and I_{3c500}PtMo's are summarized in Table 4, indicating the presence of Pt and/or Mo atoms in the materials. The XPS measurements of the materials showed peaks at 70.9–71.0 eV due to the 4f orbital of Pt and/or at 232.4–232.6 eV due to the Mo_{3d} orbital of MoO_3. The SEM–EDX analysis of the materials revealed that Pt and/or MoO_3 particles were uniformly dispersed on the surfaces of the materials. The TEM images of the materials showed the presence of particles with the diameters of a few nanometers, possibly Pt particles, and of 50–100 nm, possibly MoO_3 particles, in the matrix (Fig. 4). The oxidation–reduction reaction of an aqueous silver nitrate solution with the materials under the irradiation of visible light ($\lambda > 460$ nm) were performed and the results are shown in Table 5. The calcined materials were found to form both Ag and O_2, indicating that the materials had visible light-responsive oxidation–reduction abilities. The amounts of Ag and O_2 formed for I_{3c500}Pt (No. 2) were slightly higher than those for Pt-unloaded material I_{3c500} (No. 1), indicating that Pt-loading enhanced the photocatalysis ability. It is noted that the amounts of Ag and O_2

Table 3 Reduction activities (ra) of calcined materials I_cs

Materials	Ra (μmol × g^{-1} × h^{-1})
I_{1c400}	3.18
I_{1c500}	3.34
I_{1c600}	2.37
I_{2c400}	5.95
I_{2c500}	6.45
I_{2c600}	4.84
I_{3c400}	8.70
I_{3c500}	13.8
I_{3c600}	4.39

Table 4 Elemental analyses of Pt-loaded materials I_{3c500}Pt and I_{3c500}PtMo's

Materials	C (%)	Zr (%)	Mo (%)	Pt (%)	[C]:[Zr]:[Mo]
I_{3c500}Pt	64.46	8.35	–	0.38	59:1:–
$I_{3c500}PtMo_1$	64.56	8.89	0.89	0.53	55:1:0.1
$I_{3c500}PtMo_2$	58.85	8.19	4.35	0.43	55:1:0.5
$I_{3c500}PtMo_3$	57.26	7.68	8.86	0.39	57:1:1.1

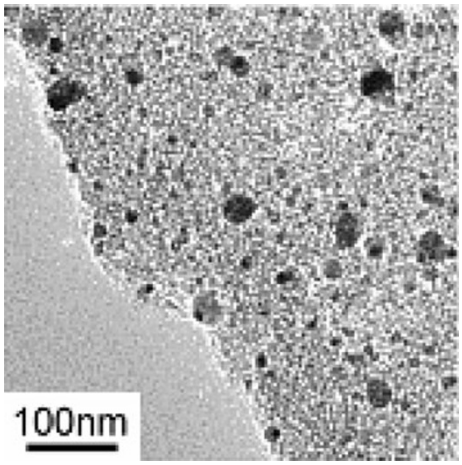

Fig. 4 TEM image of MoO_3-loaded PtI_{3c500}

formed in I_{3c500}PtMo's (Nos. 3–5) were higher than those in I_{3c500}Pt (No. 2), indicating that MoO_3-loading on the surface of I_{3c500}Pt enhanced the photo-catalysis ability. The amount of O_2 formed for I_{3c500}PtMos increased with the increase of the amount of MoO_3 in the materials, suggesting that an oxidative MoO_3 may enhance the oxidation ability of the calcined material. However, the amount of Ag formed for I_{3c500}PtMo's was found to decrease with the increase of MoO_3 in the materials. Our assumption is that MoO_3 may indiscriminately be modified on the surface of I_{3c500}Pt and thus, MoO_3 loaded at the reduction site may decrease the reduction ability at the reduction site to decrease the Ag formation. In order to

Table 5 Amounts of Ag and O_2 formed in the visible light-irradiated decomposition reaction of an aqueous $AgNO_3$ solution with the calcined materials

No	Materials	μmol × g^{-1} × h^{-1}		Ratios
		Ag	O_2	[Ag]/[O_2]
1	I_{3c500}	112	27	4.1
2	I_{3c500}Pt	117	32	3.7
3	$I_{3c500}PtMo_1$	199	95	2.1
4	$I_{3c500}PtMo_2$	182	107	1.7
5	$I_{3c500}PtMo_3$	156	120	1.3
6	I_{3c500}MoPt	92	44	2.1
7	I_{3c500}PtMn	202	140	1.4

Table 6 Water decomposition reaction with the calcined materials under the irradiation of visible light ($\lambda > 460$ nm)

No	Materials	nmol		Ratios
		H_2	O_2	[H_2]/[O_2]
1	I_{3c500}	0	0	–
2	I_{3c500}Pt	0	0	–
3	$I_{3c500}PtMo_1$	7.1	27.8	0.26
4	I_{3c500}PtMn	0	74.4	–

confirm this assumption, the surface of I_{3c500} was initially modified with MoO_3, followed by subsequent Pt-loading according to the procedure described in "MoO_3-modification on I_{3c500}" to obtain I_{3c500}MoPt. The visible-light irradiated decomposition reaction of methylene blue with I_{3c500}MoPt was examined and the results are also shown in Table 5. As expected, the amounts of both Ag and O_2 formed in I_{3c500}MoPt (No. 6) were considerably lower than those in $I_{3c500}PtMo_1$ (No. 3). The normal electrode potential (E^0) of MoO_3 is +0.32 V. Here, the loading of metal oxide with a higher E^0 value is expected to enhance the oxidation ability of the material. Thus, MnO_2 with the E^0 value of +1.23 V was modified on the surface of I_{3c500}Pt according to the procedure described in "Pt-loading on I_{3c500}Mo" and "MnO_2-loading on I_{3c500}Pt" to obtain I_{3c500}PtMn. The photo-catalysis ability of I_{3c500}PtMn was examined and the results are also shown in Table 5. The amount of O_2 formed for I_{3c500}PtMn (No. 7) was found to be higher than that for I_{3c500}PtMo's (Nos. 3–5), indicating that MnO_2 enhanced the oxidation ability. However, the amounts of Ag formed for $I_{3c500}PtMo_1$ (No. 3) and I_{3c500}PtMn (No. 7) were nearly equal, suggesting that a partial reduction of MnO_2 may take place for I_{3c500}PtMn. Water photo-decomposition examinations were performed and the results are shown in Table 6. No H_2 and O_2 evolution was observed for I_{3c500} (No. 1) and I_{3c500}Pt (No. 2). On the other hand, $I_{3c500}PtMo_1$ (No. 3) was found

to evolve both H_2 and O_2, however, the $[H_2]/[O_2]$ ratio was smaller than an ideal ratio of 2. Our consideration is that a partial reduction of MoO_3 deposited on the reduction site of the material may take place to decrease the reduction ability. Another interesting finding is that the amount of O_2 evolved for I_{3c500}PtMn (No. 4) was higher than that for $I_{3c500}PtMo_1$ (No. 3) but no H_2 evolution was observed for I_{3c500}PtMn. Higher O_2 evolution may be due to higher oxidation ability of MnO_2, as described above. Non-formation of H_2 may be due to an occurrence of reduction reaction of MnO_2 formed at the reduction site.

Conclusions

Nano-sized ZrO_2/carbon clusters composite materials denoted as I_c's were successfully synthesized by the calcination of $ZrCl_4$/starch complexes denoted as I's. Pt-loaded ZrO_2/carbon clusters composite materials were also prepared by doping the Pt particles on the surfaces of I_c's. The surfaces of the Pt-loaded materials were further modified with MoO_3 particles and the MoO_3-loaded materials thus obtained were found to show a visible light-sensitive oxidation–reduction function.

References

Aki H, Yamamoto S, Yamaguchi T, Kondoh J, Maeda T, Murata H, Ishii I (2006) Fuel cells and energy networks of electricity, heat, and hydrogen in residential areas. Int J Hydrogen Energy 31:967

Domen K, Kondo JN, Hara M, Takata T (2000) Photo- and mechano-catalytic overall water splitting reactions to form hydrogen and oxygen on heterogeneous catalysts. Bull Chem Soc Jpn 73:1307

Fujihara K, Ohno T, Matsumura M (1998) Splitting of water by electrochemical combination of two photocatalytic reactions on TiO_2 particles. J Chem Soc Faraday Trans 94:3705

Furukawa T, Matsui H, Hasegawa H, Karuppuchamy S, Yoshihara M (2007) The electronic behaviors of calcined materials from a (*S*-nickel-*S*-phenylene-*O*)–strontium -(*O*-phenylene-*S*-selenium-*S*) hybrid copolymer. Solid State Commun 142:99

Ge S, Jia H, Zhao H, Zheng Z, Zhang L (2010) First observation of visible light photocatalytic activity of carbon modified Nb_2O_5nanostructures. J Mater Chem 20:3052

Kawahara T, Kuroda T, Matsui H, Mishima M, Karuppuchamy S, Seguchi Y, Yoshihara M (2007a) Electronic properties of calcined materials from a scandium-*O*-phenylene-*O*-yttrium-*O*-phenylene hybrid copolymer. J Mater Sci 42:3708

Kawahara T, Miyazaki H, Karuppuchamy S, Matsui H, Ito M, Yoshihara M (2007b) Electronic nature of vanadium nitride–carbon cluster composite materials obtained by the calcination of oxovanadylphthalocyanine. Vacuum 81:680

Kobayashi N, Narumi T, Morita R (2005) Hydrogen Evolution from p-GaN Cathode in Water under UV Light Irradiation. Jpn J Appl Phys 44:784

Konta R, Ishii T, Kato H, Kudo A (2004) Photocatalytic activities of noble metal ion doped $SrTiO_3$ under visible light irradiation. J Phys Chem B 108:8992

Kudo A, Kato H, Tsuji I (2004) Strategies for the development of Visible-light-driven Photocatalysts for Water Splitting. Chem Lett 33:1534

Matsui H, Karuppuchamy S, Yamaguchi J, Yoshihara M (2007a) Electronic behavior of calcined materials from SnO_2 hydrosol/starch composite materials. J Photochem Photobio A Chem 189:280

Matsui H, Yamamoto S, Sasai T, Karuppuchamy S, Yoshihara M (2007b) Electronic behavior of WO_2/carbon clusters composite materials. Electrochemistry 75:345

Matsui H, Ishiko A, Karuppuchamy S, Yoshihara M (2009a) Synthesis and characterization of MoO_3/carbon clusters/ZrO_2 composite materials. J Alloy Comp 437:L33

Matsui H, Nagano S, Karuppuchamy S, Yoshihara M (2009b) Synthesis and characterization of TiO_2/MoO_3/carbon clusters composite material. Current Appl Phys 9:561

Miyazaki H, Matsui H, Nagano T, Karuppuchamy S, Ito S, Yoshihara M (2008) Synthesis and electronic behaviors of TiO_2/carbon clusters/Cr_2O_3 composite materials. Appl Surf Sci 254:7365

Miyazaki H, Matsui H, Kitakaze H, Karuppuchamy S, Ito S, Yoshihara M (2009a) Synthesis and electronic behaviors of $Ce_{0.5}Hf_{0.5}O_2$/carbon clusters composite materials. Mater Chem Phys 113:21

Miyazaki H, Matsui H, Kuwamoto T, Ito S, Karuppuchamy S, Yoshihara M (2009b) Synthesis and photocatalytic activities of MnO_2-loaded Nb_2O_5/carbon clusters composite material. Micro Meso Mater 118:518

Yamamoto S, Matsui H, Ishiyama S, Karuppuchamy S, Yoshihara M (2006) Electronic behavior of calcined material from a tantalum-O-phenylene-S- tin-S-phenylene-O hybrid copolymer. Mat Sci Eng B 135:120

Zhang Y, Tang Z, Fu X, Xu YJ (2010) TiO_2-graphene nanocomposites for gas-phase photocatalytic degradation of volatile aromatic pollutant: is TiO_2-graphene truly different from other TiO_2-carbon composite materials. ACS Nano 12:7303